A Mechanistic Study on Complexes of Type *mer*-[Cr(CO)$_3$(η^2-L–L)(σ-L–L)] (where L–L = $Ph_2PCH_2PPh_2$, $Ph_2PNHPPh_2$, or $Ph_2PNMePPh_2$) using Spectroscopic and Convolutive Electrochemical Techniques†

Adrian Blagg, Stuart W. Carr, Gary R. Cooper, Ian D. Dobson, J. Bernard Gill, David C. Goodall, Bernard L. Shaw, Norman Taylor,* and Terrence Boddington
School of Chemistry, University of Leeds, Leeds LS2 9JT

The new complexes *mer*-[Cr(CO)$_3$(η^2-L–L)(σ-L–L)] [where L–L = $Ph_2PCH_2PPh_2$ (dppm), Ph_2P-$NHPPh_2$ (dppa) or $Ph_2PNMePPh_2$ (dppma)] were synthesized by treating [Cr(CO)$_3$(C_7H_8)] (C_7H_8 = cyclohepta-1,3,5-triene) with the appropriate diphosphine. The complexes were characterized by i.r. and by ^{31}P-{^1H} and ^1H-{^{31}P} n.m.r. spectroscopy. The electrochemical and chemical oxidation of these complexes was investigated and the products identified by electrochemical techniques and by e.s.r. and i.r. spectroscopy. The one-electron oxidation of *mer*-[Cr(CO)$_3$(η^2-L–L)(σ-L–L)] gives the 17-electron chromium(I) complex *mer*-[Cr(CO)$_3$(η^2-L–L)(σ-L–L)]$^+$. These chromium(I) complexes have only limited stability and have been shown to follow two reaction pathways, disproportionation (electron transfer) as in equation (i) and intramolecular displacement of CO as in equation (ii). The rates of these reactions increase markedly from L–L = dppm to dppa or dppma. A second one-electron oxidation process [equation (iii)] has been observed but the dications are very unstable and decompose to give solvated Cr^{2+}, free diphosphine, and CO gas.

$$2\,mer\text{-}[Cr(CO)_3(\eta^2\text{-L–L})(\sigma\text{-L–L})]^+ \longrightarrow mer\text{-}[Cr(CO)_3(\eta^2\text{-L–L})(\sigma\text{-L–L})]^0 + mer\text{-}[Cr(CO)_3(\eta^2\text{-L–L})(\sigma\text{-L–L})]^{2+} \quad \text{(i)}$$

$$mer\text{-}[Cr(CO)_3(\eta^2\text{-L–L})(\sigma\text{-L–L})]^+ \longrightarrow trans\text{-}[Cr(CO)_2(\eta^2\text{-L–L})_2]^+ + CO \quad \text{(ii)}$$

$$mer\text{-}[Cr(CO)_3(\eta^2\text{-L–L})(\sigma\text{-L–L})]^+ \longrightarrow mer\text{-}[Cr(CO)_3(\eta^2\text{-L–L})(\sigma\text{-L–L})]^{2+} + e \quad \text{(iii)}$$

There has been much interest in the electrochemistry of tertiary phosphine-substituted Group 6 metal carbonyl complexes. Most work has been with mono-tertiary phosphine derivatives, *i.e.* of type [M(CO)$_x$(PR_3)$_{6-x}$], although there has also been work with tridentate phosphorus-donor ligands.[1,2] The work described in the present paper is largely concerned with the electrochemistry of complexes of type *mer*-[Cr(CO)$_3$(η^2-L–L)-(σ-L–L)] [L–L = $Ph_2PCH_2PPh_2$ (dppm), $Ph_2PNHPPh_2$ (dppa), or $Ph_2PNMePPh_2$ (dppma)] and first we summarize the previous results on the electrochemical oxidation of the tertiary phosphine-substituted tricarbonylchromium complexes.

For complexes of the type *fac*-[Cr(CO)$_3$(tridentate ligand)] two chemically reversible one-electron oxidations were reported which were assigned as in equations (1) and (2) as the *fac*

$$fac^0 \rightleftharpoons fac^+ + e \quad (1)$$

$$fac^+ \rightleftharpoons fac^{2+} + e \quad (2)$$

stereochemistry is fixed by the tridentate phosphine ligand.[3] With unidentate phosphorus-donor ligands (L) the meridional complexes *mer*-[Cr(CO)$_3$L$_3$] gave one chemically reversible and a second, chemically irreversible oxidation [equations (3) and (4)]. For the corresponding facial isomers *fac*-[Cr(CO)$_3$L$_3$],

$$mer^0 \rightleftharpoons mer^+ + e \quad (3)$$

$$mer^+ \rightleftharpoons mer^{2+} + e \quad (4)$$

$$mer^{2+} \xrightarrow{\text{fast}} \text{products}$$

† *Non-S.I. unit employed:* G = 10^{-4} T.

Scheme 1 was required to explain the electrochemical behaviour[1] on oxidation.

$$\begin{array}{ccc} fac^0 & \rightleftharpoons & fac^+ + e \\ \Updownarrow & \nearrow\!\searrow & \Updownarrow \\ mer^0 & \rightleftharpoons & mer^+ + e \end{array}$$

Scheme 1. The crossed arrows represent the cross redox reaction $fac^+ + mer^0 \rightleftharpoons fac^0 + mer^+$

We have described the synthesis of homo- and hetero-bimetallic complexes, and related mononuclear species, containing dppm and related ligands.[4] We have begun a study of the electrochemical properties of these complexes and, in the present paper, we report a study of complexes of the type *mer*-[Cr(CO)$_3$(η^2-L–L)(σ-L–L)] (L–L = dppm, dppa, or dppma). When we started this electrochemical work we were particularly interested on the effect that the unco-ordinated phosphorus atom would have on the electrochemical properties. These chromium tricarbonyl complexes are new and their synthesis and characterization is described first before the results of the electrochemical and associated studies are discussed.

Experimental

Preparations.—Operations involving tertiary phosphines were carried out under an atmosphere of dinitrogen or argon. Literature methods were used to prepare dppm,[5] dppa,[6] and dppma.[6]

mer-[Cr(CO)$_3$(dppm-*PP'*)(dppm-*P*)]·0.75CH_2Cl_2. A mixture of [Cr(CO)$_3$(C_7H_8)] (C_7H_8 = cyclohepta-1,3,5-triene) (0.2 g, 0.88 mmol) and dppm (1.0 g, 2.6 mmol) in ethanol (15 cm^3)

was heated under reflux for 30 min during which time some of the required product separated from the hot mixture. The cooled reaction mixture was evaporated to dryness under reduced pressure and the residue recrystallized from CH_2Cl_2–Et_2O to give the required product as orange-red prisms (0.66 g, 0.68 mmol, 78%), m.p. 171—174 °C (Found: C, 66.7; H, 4.7; Cl, 5.5. Calc. for $C_{53.75}H_{45.5}Cl_{0.75}CrO_3P_4$: C, 66.6; H, 4.9; Cl, 5.3%).

mer-[Cr(CO)$_3$(dppa-*PP'*)(dppa-*P*)]·0.25C_6H_6. A mixture of [Cr(CO)$_3$(C_7H_8)] (0.23 g, 1.0 mmol) and dppa (0.77 g, 2.0 mmol) in dry benzene (15 cm^3) was heated under reflux for 2 h. The mixture was then cooled and light petroleum (b.p. 40—60 °C) added and the solution cooled to *ca.* 5 °C. This gave the required product as orange microcrystals (0.85 g, 0.94 mmol, 94%) (Found: C, 67.55; H, 4.6; N, 3.1. Calc. for $C_{52.5}H_{42.5}CrN_2O_3P_4$: C, 68.05; H, 4.75; N, 3.0%). The complex *mer*-[Cr(CO)$_3$(dppma-*PP'*)(dppma-*P*)] was similarly prepared in 95% yield as orange microcrystals (Found: C, 68.1; H, 4.95; N, 3.0. Calc. for $C_{53}H_{46}CrN_2O_3P_4$: C, 67.8; H, 4.65; N, 2.85%).

cis-[Cr(CO)$_2$(dppma-*PP'*)$_2$]. A mixture of [Cr(CO)$_6$] (0.2 g, 9.1 mmol) and dppma (1.1 g, 27.3 mmol) was heated under reflux in n-decane under an N_2 atmosphere for 24 h. The solution was then cooled and the product collected. It formed orange microcrystals from benzene–n-hexane (yield 0.25 g, 2.7 mmol, 30%) (Found: C, 69.1; H, 5.1; N, 2.9. Calc. for $C_{52}H_{46}CrN_2O_2P_4$: C, 68.9; H, 5.1; N, 3.1%). The complex *cis*-[Cr(CO)$_2$(dppa-*PP'*)$_2$] was prepared similarly in 32% yield (Found: C, 67.7; H, 4.6; N, 3.2. Calc. for $C_{50}H_{42}CrN_2O_2P_4$: C, 68.3; H, 4.8; N, 3.2%).

Instrumentation.—(*a*) *Electrochemical measurements.* Cyclic linear-sweep voltammetry and chronoamperometry were performed using an E. G. and G. PAR model 363 potentiostat/galvanostat and model 175 universal programmer. The current response and applied potentials were stored on a magnetic disk *via* a fast data-capture system, based upon a twin-channel 12-bit analogue-to-digital converter (conversion time 50 μs) and a Gemini Galaxy 2 microcomputer. Data-capture software was written in Macro 80 assembler language which allowed a minimum acquisition time of 100 μs per point. In all experiments 2 000 data points were routinely captured, equally spaced in time, with a time interval appropriate to the time-scale of the particular experiment. The system thus allowed use of any scan rate up to 100 V s^{-1} for linear-sweep experiments. Background data were also stored, and were subtracted from the experimental data set, minimizing effects such as double-layer charging currents. It was found, however, that whilst very fast scan rates were practical in aqueous systems, in the solvents used for this study the faradaic-to-background current ratio was poor above 10 V s^{-1}. This scan rate was therefore taken as the practical upper limit.

The electrochemical measurements were made using a conventional three-electrode cell configuration. A selection of working electrodes was used. This included a modified PAR SDME 303 for hanging mercury drop and Metrohm inlaid platinum, gold, and glassy carbon disks, each of the disk electrodes having a geometrical surface area of around 0.2 cm^2. For most of the quantitative work the platinum electrode was used. The planar geometry simplified some of the mathematical treatments performed. The reference electrode used depended on the solvent system. In dichloromethane, Ag—AgCl in saturated LiCl—CH_2Cl_2 was chosen, whilst in dimethylformamide and acetonitrile, Ag—$AgNO_3$ was used (0.01 mol dm^{-3} $AgNO_3$ in the appropriate solvent). A 1-cm^2 platinum-sheet auxiliary electrode was used throughout. All electrochemical experiments were performed in light-proof cells. All solvents were dried over type 4A molecular sieves. All solutions were 0.1 mol dm^{-3} in tetrabutylammonium perchlorate as the background electrolyte. Solutions were purged with nitrogen before each experiment and an atmosphere of nitrogen was maintained above the working solution. Internal-resistance ohmic drop distortions were minimized by applying positive feedback compensation.

(*b*) *Electron spin resonance.* A Varian E-line e.s.r. spectrometer, operating at a microwave frequency of 9.5 GHz, was used to record all e.s.r. spectra. Chemical oxidations were performed in a quartz tube (internal diameter 3 mm). For the electrochemical oxidations, a cell was constructed inside a similar tube. Both the working and auxiliary electrodes were formed from platinum-wire spirals and were insulated using Teflon tubing. A silver wire inside a third Teflon tube was used as a pseudo-reference electrode. The working electrode was positioned so as to be in the centre of the microwave cavity whilst the auxiliary electrode was positioned just outside the cavity.

All solutions were purged with argon before use and an argon atmosphere was maintained above the solution throughout the experiment. Temperature control was possible between 20 and −70 °C by alteration of the flow rate of cooled nitrogen through the cavity (*i.e.* around the cell).

(*c*) *Infrared spectra.* These spectra were recorded using a Pye-Unicam SP-2000 i.r. spectrophotometer, calibrated against polystrene.

(*d*) *Nuclear magnetic resonance.* All n.m.r. spectra were recorded on a JEOL FX-100 spectrometer. Phosphorus-31 spectra were recorded using 85% H_3PO_4 as an external standard, proton spectra using tetramethylsilane as an internal standard.

Treatment of Electrochemical Data.—Voltammetric data tend to be difficult to handle quantitatively in their original form. Despite capturing data points covering the entire course of, say, a cyclic voltammetric experiment, it is still common to find that the analysis of such data is based upon the current and potential values of a few specific points. Often the points of peak or half-peak current are chosen, although these have in fact no special significance compared with the rest of the data throughout a linear-sweep wave. It is much more preferable to use as many data as possible for an effective analysis and a convolution-transform method has been proposed which can give simple mathematical forms to the transformed current data.[7–11] For simple electron transfer this convolution of the current data, i, with a $(\pi t)^{-\frac{1}{2}}$ function is obtained from the whole current history $i(u)$, equation (5); $I_{(t)}$ is the convoluted current at

$$I_{(t)} = i_{(t)} * \frac{1}{(\pi t)^{\frac{1}{2}}} = \frac{1}{\pi^{\frac{1}{2}}} \int_0^t \frac{i(u)}{(t-u)^{\frac{1}{2}}}\,du \qquad (5)$$

time t, u is the time. This has the distinct disadvantage for our studies in that it does not simplify the treatment of transformed data for an electron transfer followed by a chemical reaction (the so-called e.c. reaction), except at the extremes of slow and fast chemical reactions accompanying a fast electron transfer. We have developed a more general convolution for the e.c. (irreversible) case[12] which encompasses the results of Saveant[8–11] and more recently those proposed by Oldham[13] for the treatment of chronoamperometric data, and thus can be used with considerable advantage over these methods. The reaction scheme in equations (6) and (7) (R = reduced species,

$$R \underset{k_b}{\overset{k_f}{\rightleftharpoons}} O + ne \qquad (6)$$

$$O \overset{k_c}{\rightleftharpoons} P \qquad (7)$$

O = oxidized species, and P = product of the chemical step) yields relationships (8) and (9) for the concentrations of R and O

$$C_R(0,t) = C_R^{(init)} - \frac{1}{nFAD^{\frac{1}{2}}} \cdot i_{(t)} * \frac{1}{(\pi t)^{\frac{1}{2}}} = C_R^{(init)} - \frac{1}{nFAD^{\frac{1}{2}}} \cdot I_1 \quad (8)$$

$$C_O(0,t) = \frac{1}{nFAD^{\frac{1}{2}}} \cdot i_{(t)} * \frac{e^{-kct}}{(\pi t)^{\frac{1}{2}}} = \frac{1}{nFAD^{\frac{1}{2}}} \cdot I_2 \quad (9)$$

at the electrode, where n is the number of electrons transferred, A is the electrode area and D the diffusion coefficients of O and R which are assumed to be equal to simplify the equations. These relationships are quite general for all variations of the rate parameters involved. The potential is introduced *via* the Butler–Volmer relationship written in the form (10) where α is the

$$i = i_0 \left[\frac{C_R(0,t) - C_O(0,t)e^{-\xi}}{C_R^{(init)}} \right] e^{\alpha\xi} \quad (10)$$

symmetry factor, $\xi = (E - E^{\ominus})nF/RT$, and i_0 is the exchange current for the electron-transfer process at $E = E^{\ominus}$, $i_0 = nFAk_f^{\ominus}C_R^{(init)}$, $k_f^{\ominus}$ being the forward standard heterogeneous rate constant. This yields the expression (11) where I_1 and I_2 are

$$\frac{I_{(lim)}}{i_0} \cdot e^{-\alpha\xi} i = I_{(lim)} - I_1 - I_2 e^{-\xi} \quad (11)$$

the convolutions given in equations (8) and (9) respectively, and $I_{(lim)}$ [$= nFAC_R^{(init)}D^{\frac{1}{2}}$] is the limit of I as E approaches infinity. This relationship between current, voltage, and the other parameters holds for all regimes of rates of the electron transfer and the chemical reaction and in principle is suitable for treatment of data obtained *via* a wide variety of techniques. The various requirements for the determination of mechanism and calculation of the individual parameters are best satisfied by suitable selections of experiments including the use of a wide range of temperature to vary the relative importance of chemical and electron-transfer processes. Cyclic voltammetry is without doubt most important in the determination of mechanism and the measurement of the current peaks, *etc.* may give an early indication, for example, of chemical reactions or regenerative processes following the electron-transfer step. After suitable adjustments of sweep rate and temperature to make the contribution of the chemical reaction negligible, checks for reversibility, quasi-reversibility, or irreversibility of the electron transfer could be carried out on the convoluted data, using an expression stemming from equation (11) appropriate for the i_0 regime of the particular class of electron transfer.

Absence of chemical processes was in general indicated in cyclic voltammetric experiments by the return of I_1 to zero on completion of a full cycle. Logarithmic checks on the data could be applied and in principle the appropriate values of the various parameters could be extracted from this treatment. Tests for reversibility always included an assessment of the overlay of the 'forward and backward' convoluted currents. Here the display of the third differential of I_1 was found to be extremely useful and was used as a standard procedure. The construction proposed by Saveant and Tessier[11] was used to determine E in the quasi-reversible case from the cyclic voltammetry experiments, but it was found more satisfactory to determine this and the other parameters from chronamperometric experiments (see later). In the presence of chemical reactions, equation (12) could be derived from (11). It is somewhat unwieldy in view of the values of the parameters which must be known *a priori* but

$$-\frac{(E - E^{\ominus})}{RT} nF = \ln \left[\frac{I_{(lim)} - I_1}{I_2 + (D^{\frac{1}{2}}/k_f^{\ominus})ie^{(1-\alpha)\xi}} \right] \quad (12)$$

in the case of fast electron transfer (large i_0) the expression reduces to (13) where only k_c is required. Tests on simulated

$$-\frac{(E - E^{\ominus})}{RT} nF = \ln \left[\frac{I_{(lim)} - I_1}{I_2} \right] \quad (13)$$

data[12] showed that inappropriate k_c values gave quite large deviations of the log plot from linearity, particularly on the reverse sweep. Alternatively the crossing points of $[I_{(lim)} - I_1]$ and I_2 on the forward and particularly on the reverse sweep were displaced from $E_{\frac{1}{2}}$ except for convolution with the accurate value of k_c. The usual experimental procedure was to adjust the sweep rate until I_1 returned to 20—60% of $I_{(lim)}$ at the end of the sweep. The difference in voltage at the crossing points was then a sensitive function of the k_c value used in the convolution to give I_2. At this stage convolution is only required in the vicinity of $E^{\ominus}$. The $D^{\frac{1}{2}}$ values were obtained from $I_{(lim)}$ using equations (8) and (9).

Chronoamperometric experiments were used extensively to determine various parameters. With constant applied potential, E, a linear relationship is established between the current and the sum of I_1 and $I_2[\exp(-\xi)]$. This general relationship contains the particular forms obtained by Oldham[13] and extends to any variation of the parameters. Equation (11) may be written in the form (14). In the absence of chemical reaction

$$i = I_{(lim)} \cdot \frac{k_f}{D^{\frac{1}{2}}} - \left(\frac{k_f}{D^{\frac{1}{2}}} \cdot I_1 + \frac{k_b}{D^{\frac{1}{2}}} I_2 \right) \quad (14)$$

(*i.e.* $I_1 = I_2$) the following conclusions can be derived from equation (14). For fast electron transfer the intercept approaches infinity as I_1 and I_2 approach zero, *i.e.* the bracketted sum in equation (14) is independent of i. This constancy of I_1 [equal to $I_{(lim)}$] is equivalent to adherence to the Cottrell relationship. In the quasi-reversible case, experiments at large voltage steps yielded D *via* measurements of $I_{(lim)}$ and this then yielded k_f from the intercept and k_b from the use of an intercept and slope [equation (14)].

The equality of k_f and k_b at $E_{\frac{1}{2}}$ was used to obtain the $E_{\frac{1}{2}}$ value (see Figure 1).

The symmetry factor (α) was obtained from log plots of k_f and k_b in the vicinity of $E_{\frac{1}{2}}$. The variation in α at extremes of potential is probably due to the fall in potential across the outer Helmholtz layer. In the presence of chemical reactions, appropriate expressions can be extracted from equation (11).

Results and Discussion

Preparation of the Complexes.—The complex *mer*-[$Cr(CO)_3$(dppm-*PP'*)(dppm-*P*)] was prepared by treating [$Cr(CO)_3(C_7H_8)$] with dppm in hot ethanol. There was no sign of the intermediate formation of the corresponding *fac* isomer, in contrast with the behaviour of the analogous molybdenum or tungsten complexes, [$M(CO)_3(C_7H_8)$] from which the *fac* isomers, [$M(CO)_3$(dppm-*PP'*)(dppm-*P*)], are formed first.[4,14] Details of the preparation and elemental analytical data are given in the Experimental section and characterizing i.r. and ^1H-{^{31}P} and ^{31}P-{^1H} n.m.r. data are given in Table 1 and discussed below. We similarly prepared and characterized the corresponding dppa and dppma complexes. We have also prepared and characterized *cis*-[$Cr(CO)_2$(dppa-*PP'*)$_2$] and *cis*-[$Cr(CO)_2$(dppma-*PP'*)$_2$] by heating [$Cr(CO)_6$] with 2 mol of dppa or dppma (respectively) in refluxing n-decane, see Experimental section and Table 1 for further details and characterization data.

In the i.r. spectra of the tricarbonyl complexes the presence of

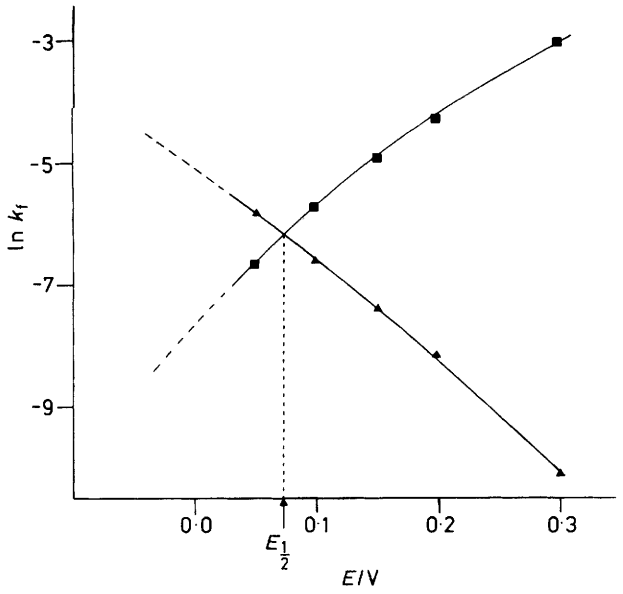

Figure 1. Plots of ln k_f (■) and ln k_b (▲) against potential (V *vs.* Ag—AgCl in dichloromethane) for the electron-transfer reaction (at −65 °C) *mer*-$[Cr(CO)_3(dppm\text{-}PP')(dppm\text{-}P)]$ $\underset{k_b}{\overset{k_f}{\rightleftharpoons}}$ *mer*-$[Cr(CO)_3(dppm\text{-}PP')(dppm\text{-}P)]^+$ + e. A platinum working electrode was used

three strong (or medium) bands in the region due to CO stretch is indicative of a *mer* configuration (see Table 1). For *mer*-$[Cr(CO)_3(dppm\text{-}PP')(dppm\text{-}P)]$ a singlet at δ = 4.44 p.p.m. in the $^1H\text{-}\{^{31}P\}$ n.m.r. spectrum is indicative of the dppm-*PP'* CH_2 protons being similar in chemical shift to the CH_2 protons of $[Cr(CO)_4(dppm\text{-}PP')]$. The other resonance, at δ = 2.95 p.p.m., is assigned to the CH_2 protons of unidentate dppm. The resonances due to the NH proton of dppa, at δ 4.7 and 3.3 p.p.m., were similarly assigned. The assignments of the CH_3 resonances to dppma-*PP'* or dppma-*P* are less definite.

In the $^{31}P\text{-}\{^1H\}$ n.m.r. spectrum of *mer*-$[Cr(CO)_3(dppm\text{-}PP')(dppm\text{-}P)]$ a doublet at δ = −26 p.p.m. is assigned to the uncomplexed phosphorus nucleus of the unidentate dppm ligand: the resonance of uncomplexed dppm is at −22 p.p.m. The doublet at δ = −26 p.p.m., due to P(D) (Table 1), shows a *J*(PP) coupling at 37 Hz clearly due to coupling with P(C); this enables the resonance at δ = 65 p.p.m. (doublet of doublet of doublets) to be assigned to P(C). The doublet of doublet patterns at δ = 26 or 50 p.p.m. (Table 1) are therefore assigned to P nuclei (A) or (B) but we do not know which is which. Similar arguments were applied to the assignments of the resonances of the dppa complex. Somewhat surprisingly each of the resonances of the P nuclei in *mer*-$[Cr(CO)_3(dppma\text{-}PP')(dppma\text{-}P)]$ occurs as a doublet of doublet of doublets. The resonance at δ = 54 p.p.m. is assigned to P(D), the uncomplexed phosphorus nucleus, being similar in chemical shift to the free

Table 1. I.r. (cm^{-1}),[a] $^{31}P\text{-}\{^1H\}$ n.m.r. and $^1H\text{-}\{^{31}P\}$ n.m.r. data

Complex	ν(CO)	δ(P)[b]	Assignment[c]	*J*(P–P)[d]	δ(H)[e] (non-aromatic) unidentate	δ(H)[e] (non-aromatic) chelate
mer-$[Cr(CO)_3(dppm\text{-}PP')(dppm\text{-}P)]$	1 951m	−26(d)	D	37 (C–D)	2.95	4.44
	1 860s	65(ddd)	C	37, 18, 27		
		26(dd)	A(B)	27, 3		
		50(dd)	B(A)	18, 3		
mer-$[Cr(CO)_3(dppa\text{-}PP')(dppa\text{-}P)]$[f]	1 960s	26(d)	D	9 (C–D)	3.3	4.7
	1 860s	120(ddd)	C	30, 23, 9		
		95(dd)	A(B)	38, 30		
		114(dd)	B(A)	38, 23		
mer-$[Cr(CO)_3(dppma\text{-}PP')(dppma\text{-}P)]$	1 947s	54(ddd)	D	181 (C–D)	2.27	2.39
	1 850s	147(ddd)	C	42, 9		
	1 845s	110(ddd)	A(B)	181, 26, 17		
		130(ddd)	B(A)	54, 42, 26		
				54, 17, 9		
cis-$[Cr(CO)_2(dppma\text{-}PP')_2]$[g]	1 844s	129, 108		'N' = 69		2.54
	1 784s					2.48
cis-$[Cr(CO)_2(dppa\text{-}PP')_2]$[g]	1 840s	110, 91		'N' = 68		4.8
	1 788s					

[a] Spectra recorded as Nujol mulls. [b] Recorded at 40.25 MHz; δ values (±0.5 p.p.m.) to high frequency of H_3PO_4. d = Doublet, dd = doublet of doublets, ddd = doublet of doublet of doublets. [c] A = P_A, *etc.* A(B) or B(A) indicates either to P_A or P_B, see Discussion. P_A, P_B, P_C, and P_D are as in the structure below.

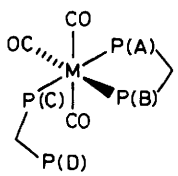

[d] C–D ≡ $^2J(P_C\text{–}P_D)$. The values are readily extracted from the d, dd, or ddd patterns. [e] Recorded at 100 MHz; δ values (±0.01 p.p.m.) to high frequency of $SiMe_4$. [f] ν(NH) at 3 340w and 3 300w cm^{-1} [g] The four phosphorus nuclei make up an AA'XX' spin system and 'N' = $^2J(AX) + {}^4J(AX')$.

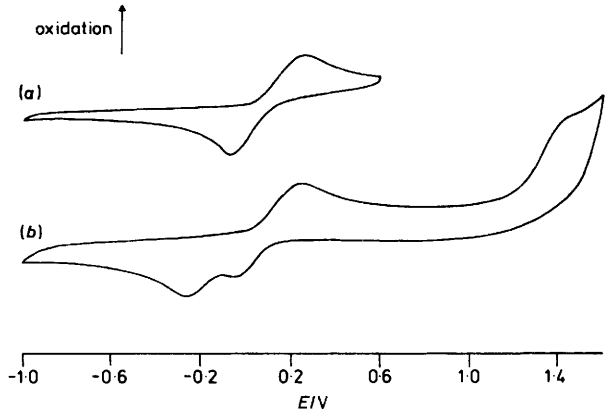

Figure 2. Cyclic voltammograms for the oxidation of *mer*-[Cr(CO)$_3$(dppm-*PP'*)(dppm-*P*)] in dichloromethane at −65 °C (scan rate 0.1 V s^{-1}): (*a*) showing the first oxidation and (*b*) with the second oxidation included

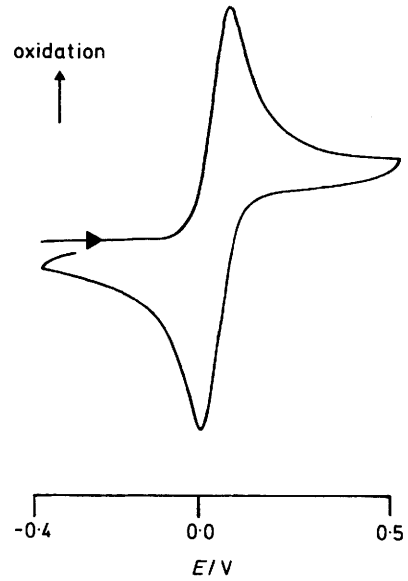

Figure 3. Cyclic voltammogram for the oxidation of *mer*-[Cr(CO)$_3$(dppm-*PP'*)(dppm-*P*)] in dichloromethane at a platinum electrode at 20 °C (scan rate 0.1 V s^{-1})

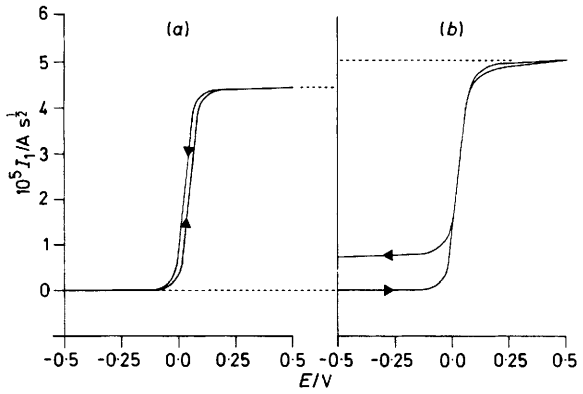

Figure 4. Plots of the convoluted current, I_1, against potential (measured against Ag—AgCl in dichloromethane) for the complex *mer*-[Cr(CO)$_3$(dppm-*PP'*)(dppm-*P*)] at a platinum electrode. The temperature was 20 °C and the scan rates were 1.0 (*a*) and 0.05 V s^{-1} (*b*)

phosphine (73 p.p.m.). This resonance shows a coupling with the remarkably high value of 181 Hz and two others, of 42 and 9 Hz (Table 1). We assign the resonance at 147 p.p.m. to P(C) having the highest chemical shift of the four P nuclei, as does P(C) in the dppm and dppa complexes, and also showing a coupling of 181 Hz, which we therefore assign to $J(P_C–P_D)$; we cannot explain why the value (181 Hz) is so high.

Electrochemistry of the Complexes.—The electrochemistry of the complexes *mer*-[Cr(CO)$_3$(η^2-L–L)(σ-L–L)] was similar so only the dppm derivative will be considered in detail. As expected, none of the complexes showed reductive behaviour before the solvent limit (−1.2 V *vs.* Ag—AgCl in dichloromethane).

(*i*) *mer*-[Cr(CO)$_3$(dppm-*PP'*)(dppm-*P*)] *at* −65 °C. Figure 2(*a*) shows a cyclic voltammogram for the first oxidation of *mer*-[Cr(CO)$_3$(dppm-*PP'*)(dppm-*P*)]. Convolution analysis of a series of cyclic voltammetric scans obtained using scan rates between 0.02 and 1 V s^{-1} confirmed that the behaviour observed is consistent with the quasi-reversible electron-transfer process (15). The virtual absence of other processes on the electro-

$$mer\text{-}[Cr(CO)_3(dppm\text{-}PP')(dppm\text{-}P)] \rightleftharpoons mer\text{-}[Cr(CO)_3(dppm\text{-}PP')(dppm\text{-}P)]^+ + e \quad (15)$$

chemical time-scale was established from the observation that the convoluted current reaches the same plateau value, regardless of the scan rate, and consistently returns, during the reverse half of the sweep, to its initial (zero) value. This shows complete conservation of the starting material within the course of the cycle. The behaviour at platinum, gold, and mercury working electrodes showed no significant differences either in dichloromethane or dimethylformamide solution, indicating that the processes observed did not involve either the solvent or the electrode material.

A second one-electron oxidation wave was observed with an oxidation peak potential 1.14 V positive of that of the first oxidation potential [Figure 2(*b*)]. No reverse (reduction) peak was observed for scan rates below 5 V s^{-1} and the process can thus be written as in equations (16) and (17). Observation of a small reverse peak at a scan rate of 10 V s^{-1} allowed the half-life

$$mer\text{-}[Cr(CO)_3(dppm\text{-}PP')(dppm\text{-}P)]^+ \rightleftharpoons mer\text{-}[Cr(CO)_3(dppm\text{-}PP')(dppm\text{-}P)]^{2+} \quad (16)$$

$$mer\text{-}[Cr(CO)_3(dppm\text{-}PP')(dppm\text{-}P)]^{2+} \xrightarrow{fast} \text{products} \quad (17)$$

of the *mer*-[Cr(CO)$_3$(dppm-*PP'*)(dppm-*P*)]$^{2+}$ species to be estimated as less than 25 ms at −65 °C at a concentration of 1.0×10^{-3} mol dm^{-3}. This behaviour is not unusual for chromium(II) carbonyl compounds[1] although the one-electron oxidation (18) was observed to be chemically reversible on the electrochemical time-scale at −75 °C.[15]

$$cis\text{-}[Cr(CO)_2(dppm\text{-}PP')_2]^+ \rightleftharpoons cis\text{-}[Cr(CO)_2(dppm\text{-}PP')_2]^{2+} + e \quad (18)$$

It was noted that after sweeping through the 1+/2+ oxidation wave a new reduction wave appeared at *ca.* −0.27 V (in dichloromethane) [Figure 2(*b*)]. This wave will be discussed later.

(*ii*) *mer*-[Cr(CO)$_3$(dppm-*PP'*)(dppm-*P*)] *at room temperature* (20 °C). Figure 3 shows a cyclic voltammogram of the first oxidation of *mer*-[Cr(CO)$_3$(dppm-*PP'*)(dppm-*P*)] at 20 °C. There is little difference apparent compared with the behaviour at −65 °C, except for faster electron transfer. Convolution analysis allows a better qualitative examination of the system

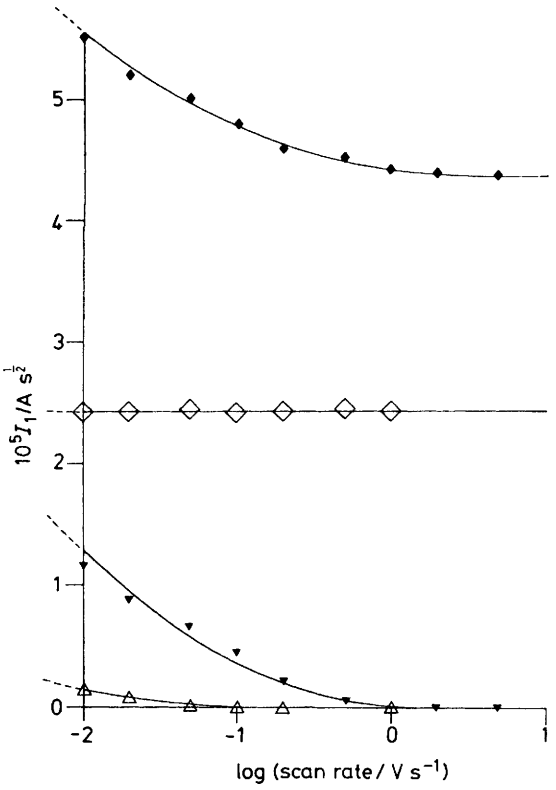

Figure 5. Plots of the limiting [$I_{(lim)}$] and final [$I_{(final)}$] values of the convoluted current (I_1) as a function of the scan rate for a series of oxidative cyclic voltammograms of *mer*-[$Cr(CO)_3$(dppm-*PP'*)(dppm-*P*)] at a platinum electrode: (◆) $I_{(lim)}$ at 20 °C, (▼) $I_{(final)}$ at 20 °C, (◇) $I_{(lim)}$ at −65 °C, and (△) $I_{(final)}$ at −65 °C

and in fact there exist correlations between the plateau value of the convoluted current (I_1) and the scan rate employed as shown in Figure 4. Similarly a correlation is found between the final value taken by the convoluted current (I_1) and the scan rate (Figures 4 and 5). This behaviour is consistent with some disproportionation of the species *mer*-[$Cr(CO)_3$(dppm-*PP'*)(dppm-*P*)]$^+$ [equation (19)]. On the forward sweep, the

$$2\ mer\text{-}[Cr(CO)_3(dppm\text{-}PP')(dppm\text{-}P)]^+ \longrightarrow mer\text{-}[Cr(CO)_3(dppm\text{-}PP')(dppm\text{-}P)] + mer\text{-}[Cr(CO)_3(dppm\text{-}PP')(dppm\text{-}P)]^{2+} \quad (19)$$

regeneration of [$Cr(CO)_3$(dppm-*PP'*)(dppm-*P*)] is responsible for enhancing the currents, the degree of enhancement being dependent upon the time spent forming *mer*-[$Cr(CO)_3$(dppm-*PP'*)(dppm-*P*)]$^+$. On the reverse sweep we observe reduction of *mer*-[$Cr(CO)_3$(dppm-*PP'*)(dppm-*P*)]$^+$. As a consequence of the disproportionation, the reductive convoluted wave has lower amplitude than the oxidative convoluted wave.

As we have already noted, *mer*-[$Cr(CO)_3$(dppm-*PP'*)(dppm-*P*)]$^{2+}$ shows practically no stability on the electrochemical time-scale even at −65 °C and consequently is expected to react further immediately.

A ^{31}P n.m.r. study of a solution of *mer*-[$Cr(CO)_3$(dppm-*PP'*)(dppm-*P*)] oxidized at a potential of +1.4 V in dichloromethane showed only a singlet at δ −22.5 p.p.m. which is characteristic of unco-ordinated dppm.

(*iii*) *Chemical oxidation of mer*-[$Cr(CO)_3$(dppm-*PP'*)(dppm-*P*)]. As predicted from the electrochemistry, $AgClO_4$ readily oxidized the compound *mer*-[$Cr(CO)_3$(dppm-*PP'*)(dppm-*P*)] and this oxidation was accompanied by a colour change from orange to brick-red and the deposition of a silver mirror. Immediately after oxidation a reductive cyclic voltammogram was observed to be identical with the oxidative voltammogram of *mer*-[$Cr(CO)_3$(dppm-*PP'*)(dppm-*P*)], implying that no fast structural change occurs on oxidation, *i.e.* the oxidized complex retains the *mer* stereochemistry. Over a period of a few minutes, evolution of carbon monoxide was observed and additional redox behaviour became evident (see below).

(*iv*) *An e.s.r. study of mer*-[$Cr(CO)_3$(dppm-*PP'*)(dppm-*P*)]$^+$. (*a*) *At low temperature* (−65 °C). The complex *mer*-[$Cr(CO)_3$(dppm-*PP'*)(dppm-*P*)] was oxidized in the e.s.r. spectrometer microwave cavity, both electrochemically and chemically (using $AgClO_4$). The resulting e.s.r. spectrum was monitored and it was found that using either method of oxidation the same spectrum was observed. The spectrum consisted of a broad quartet with intensities in the ratio 1:3:3:1 and changing the temperature did little to alter the linewidth. The compound *mer*-[$Cr(CO)_3$(dppm-*PP'*)(dppm-*P*)]$^+$ would be expected to give a doublet of doublets of doublets, due to coupling to three inequivalent phosphorus atoms directly bonded to the chromium. The observed 1:3:3:1 hyperfine structure arises because the signal is broad and the hyperfine coupling constants to the phosphorus atoms are expected to be similar. It is possible that the broadening could also be due to further unresolved coupling to the methylene protons of the dppm ligands. The similarity of the hyperfine coupling constants implies that the unpaired spin density is approximately equal on each of the directly bonded phosphorus atoms. The $\langle g \rangle$ value for *mer*-[$Cr(CO)_3$(dppm-*PP'*)(dppm-*P*)]$^+$ was 2.012 and the average hyperfine splitting was 23.0 ± 1 G. The closeness of the measured $\langle g \rangle$ value to the free-spin value suggests that the spectrum is due to a spherically symmetric state and so must be d^5 (low-spin) chromium(I).

A number of processes can be responsible for line broadening in e.s.r. spectroscopy, including rapid chemical reaction, fast spin–lattice relaxation, and nuclear quadrupole interaction. It has been found that, for complexes of the type *mer*-[$Cr(CO)_3L_3$] (where L = a unidentate phosphine ligand) and [$Cr(CO)_3$(arene)], e.s.r. line broadening occurs due to a fast electron-exchange process of the type (20) provided that there is no gross structural change.[1,16,17]

No such process was identified in our study despite the fact that the self-exchange reaction is virtually certain to occur. When the heterogeneous electron-transfer rate of the 0/1+ redox couple is considered, then it became apparent that, assuming the same mechanism of electron transfer to occur as

$$Cr^{*0} + Cr^+ \rightleftharpoons Cr^{*+} + Cr^0 \quad (20)$$

at the electrode, it would be very unlikely for such exchange broadening to be visible, since according to the theory of Marcus[18] the heterogeneous and homogeneous electron-transfer rates are related approximately[19] by k(heterogeneous) = [k(homogeneous)/1 000]$^{\frac{1}{2}}$. At the highest practical concentration of the *mer*^{0} species (around 0.1 mol dm^{-3}), broadening should only be about 1×10^{-2} G based upon this theory.

(*b*) *At* 20 °C. A solution of *mer*-[$Cr(CO)_3$(dppm-*PP'*)(dppm-*P*)]$^+$ was produced by electrolysis at −65 °C where the spectrum of *mer*-[$Cr(CO)_3$(dppm-*PP'*)(dppm-*P*)]$^+$ was observed to remain unchanged over a period of several hours. After allowing the solution to warm to room temperature, spectra were taken at 10 min intervals over a period of 100 min (Figure 6). It is apparent that the initial quartet decays to a quintet in the intensity ratio 1:4:6:4:1, having a $\langle g \rangle$ value of 2.004 and a hyperfine splitting of 28.5 ± 1 G. This signal is

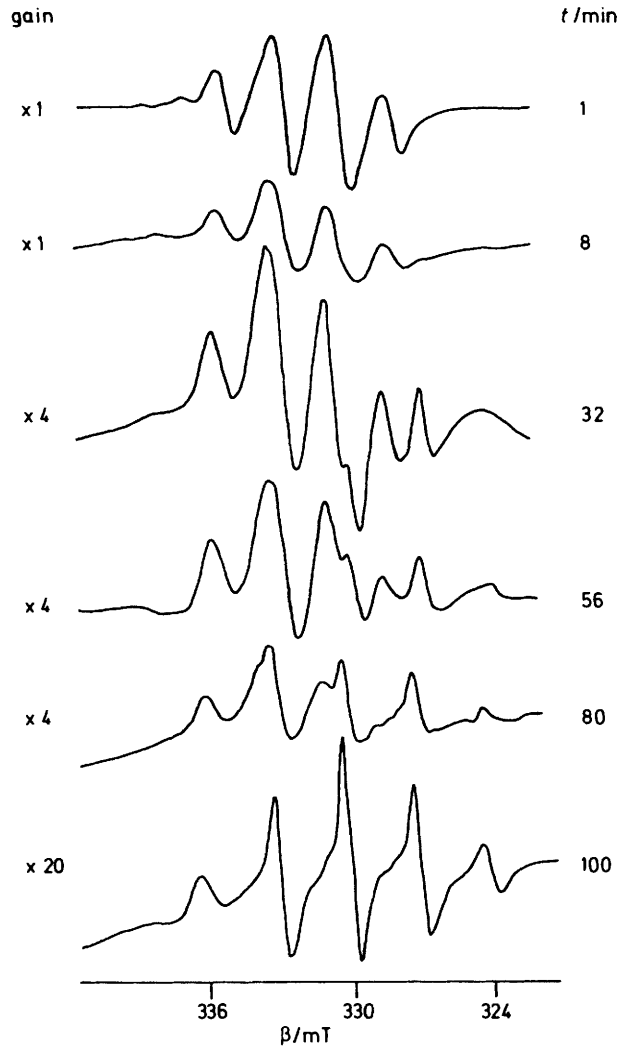

Figure 6. A series of e.s.r. spectra obtained from a solution, initially of the complex *mer*-$[Cr(CO)_3(dppm\text{-}PP')(dppm\text{-}P)]^+$ in dichloromethane at 20 °C, showing the decay with time to the species *trans*-$[Cr(CO)_2(dppm\text{-}PP')_2]^+$

identical with that given by an authentic sample of the complex *trans*-$[Cr(CO)_2(dppm\text{-}PP')_2]^+$.[20] The intramolecular displacement reaction (21) is consistent with the above observations.

$$mer\text{-}[Cr(CO)_3(dppm\text{-}PP')(dppm\text{-}P)]^+ \longrightarrow trans\text{-}[Cr(CO)_2(dppm\text{-}PP')_2]^+ + CO \quad (21)$$

However, the signal observed for *trans*-$[Cr(CO)_2(dppm\text{-}PP')_2]^+$ is only around 10% of the intensity of that of the initial *mer*-$[Cr(CO)_3(dppm\text{-}PP')(dppm\text{-}P)]^+$, and presumably disproportionation accounts for the majority of the decay of *mer*-$[Cr(CO)_3(dppm\text{-}PP')(dppm\text{-}P)]^+$.

The only e.s.r. signal remaining after 90 min is that of *trans*-$[Cr(CO)_2(dppm\text{-}PP')_2]^+$ and this signal was stable for more than 24 h.

(*v*) *The i.r. characterization of* *mer*-$[Cr(CO)_3(dppm\text{-}PP')(dppm\text{-}P)]^+$. The stability of the oxidized chromium complex $[Cr(CO)_3(dppm\text{-}PP')(dppm\text{-}P)]^+$ over a period of minutes enabled it to be characterized by i.r. spectroscopy. Oxidation with either $NOBF_4$ or $AgClO_4$ in dichloromethane initially gave an i.r. spectrum with three bands in the carbonyl region (2 036m, 1 972m, and 1 912s cm^{-1}). These data are consistent with the formation of a 17-electron *mer* isomer with C_{2v} symmetry.[1,21] The shift of the i.r. bands of the carbonyl ligands to higher frequency in the 17e complex relative to the 18e complex is of similar magnitude to those reported for the related *mer*-$[Cr(CO)_3L_3]^+$ complexes. On leaving the solution to stand for about 10 min the total intensity of the spectrum decreased and bands assignable to *trans*-$[Cr(CO)_2(dppm\text{-}PP')]^+$ and *mer*-$[Cr(CO)_3(dppm\text{-}PP')(dppm\text{-}P)]$ were observed. This behaviour is consistent with the electrochemical and e.s.r. data described above. Attempts to observe the 17e complexes *mer*-$[Cr(CO)_3(\eta^2\text{-}L\text{-}L)(\sigma\text{-}L\text{-}L)]^+$ (L–L = dppa or

Table 2. The $E_{\frac{1}{2}}$ and k^s values for the complexes *mer*-$[Cr(CO)_3(\eta^2\text{-}L\text{-}L)(\sigma\text{-}L\text{-}L)]$ and *cis*- and *trans*-$[Cr(CO)_2(\eta^2\text{-}L\text{-}L)_2]$ measured at −65 °C

Complex	$E_{\frac{1}{2}}$[a]/V	k^s/cm s^{-1}
mer-$[Cr(CO)_3(\eta^2\text{-}L\text{-}L)(\sigma\text{-}L\text{-}L)]$		
L–L = dppm	+0.075	2.0×10^{-3}
dppa	+0.160	9.0×10^{-4}
dppma	+0.093	1.4×10^{-4}
cis-$[Cr(CO)_2(\eta^2\text{-}L\text{-}L)_2]$		
L–L = dppm	−0.17	—
dppa	−0.11	1.9×10^{-1}
dppma	−0.21	2.8×10^{-3}
dppe	−0.16[b]	—
trans-$[Cr(CO)_2(\eta^2\text{-}L\text{-}L)_2]$		
L–L = dppm	−0.81	—
dppa	−0.46	6.6×10^{-2}
dppma	−0.57	1.0×10^{-2}
dppe	−0.60[b]	—

[a] Refers to the oxidation $Cr^0 \rightarrow Cr^I$, *i.e.* the $mer^{+/0}$, $cis^{+/0}$, and $trans^{+/0}$ redox couples. [b] Calculated from values quoted in ref. 22.

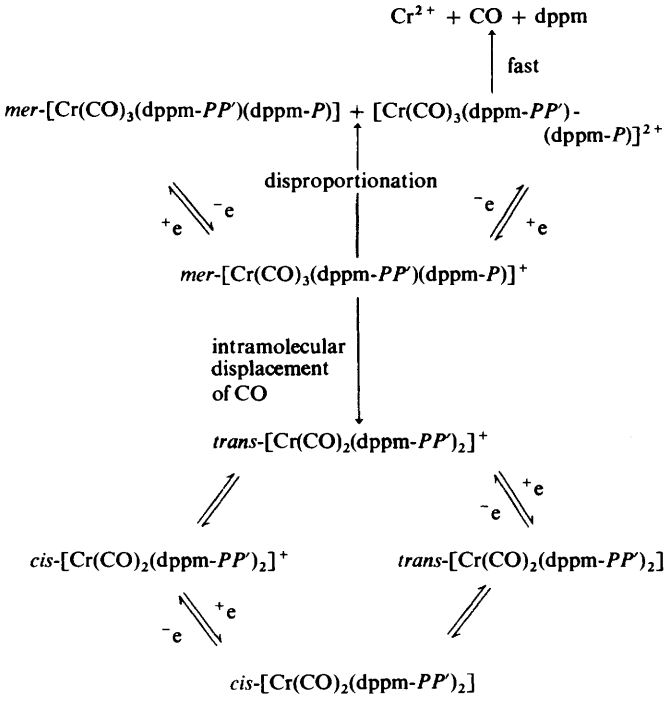

Scheme 2. A summary of the pathways which occur following electrochemical oxidation of *mer*-$[Cr(CO)_3(dppm\text{-}PP')(dppm\text{-}P)]$ as derived from electrochemical and spectroscopic measurements

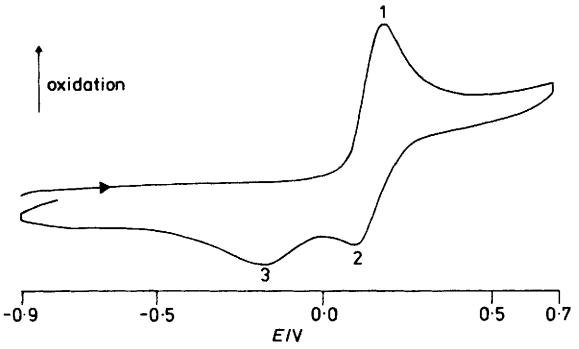

Figure 7. Cyclic voltammogram for the oxidation of the complex *mer*-$[Cr(CO)_3(dppa\text{-}PP')(dppa\text{-}P)]$ in dichloromethane at 20 °C (scan rate 0.1 V s^{-1}). Electrode processes are numbered as in the text

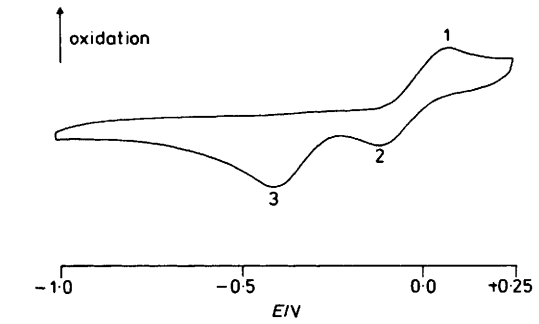

Figure 8. Cyclic voltammogram for the oxidation of the complex *mer*-$[Cr(CO)_3(dppma\text{-}PP')(dppma\text{-}P)]$ in dichloromethane at −65 °C (scan rate 0.1 V s^{-1}). Electrode processes are numbered as in the text

dppma) were unsuccessful because of the transient nature of the mer^+ complexes (see later). Scheme 2 summarizes the pathways which occur following electrochemical oxidation of *mer*-$[Cr(CO)_3(dppm\text{-}PP')(dppm\text{-}P)]$ as derived from the electrochemical and spectroscopic measurements, and the $E_{\frac{1}{2}}$ values and heterogeneous electron-transfer rates are summarized in Table 2.

(*vi*) *Electrochemical and e.s.r. study of mer*-$[Cr(CO)_3(dppa\text{-}PP')(dppa\text{-}P)]$. (*a*) *Electrochemistry.* The oxidative cyclic voltammetric behaviour of *mer*-$[Cr(CO)_3(dppa\text{-}PP')(dppa\text{-}P)]$ at 20 °C (0.1 V s^{-1}) is shown in Figure 7. The peaks numbered 1 and 2 are assigned to the $mer^{+/0}$ redox couple. Peak 3 is analogous to that obtained from *mer*-$[Cr(CO)_3(dppm\text{-}PP')(dppm\text{-}P)]$ after sweeping through the second oxidative wave and is due to a decomposition product arising from the species $[Cr(CO)_3(dppa\text{-}PP')(dppa\text{-}P)]^{2+}$. It is shifted by about 50 mV compared with the above analogue in the same solvent system (either dichloromethane or dimethylformamide) and so it seems highly probable that at least one phosphine ligand remains associated with the species responsible for the wave. The peak appeared despite the fact that the second oxidative wave was not encompassed within the cyclic voltammetric sweep. Its appearance is attributed to the decomposition of $[Cr(CO)_3(dppa\text{-}PP')(dppa\text{-}P)]^{2+}$ formed *via* a disproportionation reaction [analogous to equation (19)]. At faster scan rates the proportion of the disproportionation reaction was decreased and the wave due to $mer^+ \longrightarrow mer^0$ reduction was enhanced.

Convolution analysis of the oxidative cyclic linear-sweep behaviour of the complex *mer*-$[Cr(CO)_3(dppa\text{-}PP')(dppa\text{-}P)]$ at −65 °C indicated that even at this low temperature a certain degree of disproportionation occurs. The dependence of the plateau value of the convoluted current upon scan rate at

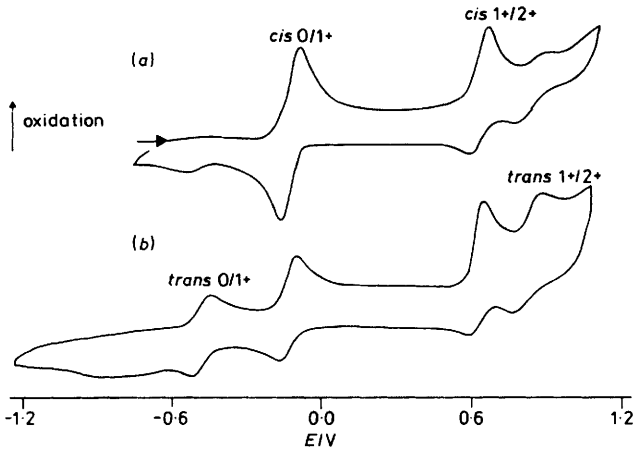

Figure 9. Cyclic voltammograms for the oxidation of *cis*-$[Cr(CO)_2(dppma\text{-}PP')_2]$ in dichloromethane at −65 °C (scan rate 0.2 V s^{-1}) showing (*a*) the first cycle and (*b*) the 20th cycle

−65 °C was very similar to that shown by *mer*-$[Cr(CO)_3(dppm\text{-}PP')(dppm\text{-}P)]$ at 20 °C.

(*b*) *E.s.r.* Electrochemical or chemical oxidation ($AgClO_4$) of *mer*-$[Cr(CO)_3(dppa\text{-}PP')(dppa\text{-}P)]$ initially gave an e.s.r. spectrum at −65 °C which was similar in appearance to that described above for the dppm analogue, that is, a broad quartet with intensities in the ratio 1:3:3:1 with a $\langle g \rangle$ value of 2.027 and a hyperfine splitting of 24.5 ± 2 G. Over a period of half an hour at −65 °C the spectrum changed to a quintet in the ratio 1:4:6:4:1. This five-line e.s.r. spectrum was identical to that produced by chemical oxidation of an authentic sample of $[Cr(CO)_2(dppa\text{-}PP')_2]$. The dicarbonyl complex had a $\langle g \rangle$ value of 2.005 and a hyperfine splitting of 29.5 ± 1 G. Oxidation of *mer*-$[Cr(CO)_3(dppa\text{-}PP')(dppa\text{-}P)]$ at room temperature resulted in the spectrum due to *trans*-$[Cr(CO)_2(dppa\text{-}PP')_2]^+$ only.

(*vii*) *mer*-$[Cr(CO)_3(dppma\text{-}PP')(dppma\text{-}P)]$. The oxidative cyclic voltammogram of *mer*-$[Cr(CO)_3(dppma\text{-}PP')(dppma\text{-}P)]$ at −65 °C is shown in Figure 8. Using a range of scan rates, the peaks numbered 1 and 2 were assigned to the $mer^{+/0}$ redox couple. Peak 3 again appears to be a decomposition product of the unstable $[Cr(CO)_3(dppma\text{-}PP')(dppma\text{-}P)]^{2+}$ species. The presence of at least one co-ordinated phosphine ligand is again suspected as peak 3 appears at a slightly different potential to its equivalent in the two compounds previously discussed.

Oxidation with $AgClO_4$ in dichloromethane at −65 °C produced a brick-red solution which decayed in minutes to leave a pale green solution. A satisfactory e.s.r. signal for the brick-red solution could not be obtained because of its rapid decomposition but it is believed to contain the complex *mer*-$[Cr(CO)_3(dppma\text{-}PP')(dppma\text{-}P)]^+$.

(*viii*) *cis*-$[Cr(CO)_2(\eta^2\text{-L–L})_2]$. To understand fully the behaviour of the tricarbonyl complexes discussed above it was essential to prepare samples of the corresponding dicarbonyl complexes. Consequently it seemed pertinent to study the electrochemistry of the complexes *cis*-$[Cr(CO)_2(\eta^2\text{-L–L})_2]$ (L–L = dppa or dppma) as these have not been previously studied.

It has been shown that $[Cr(CO)_2(dppm\text{-}PP')_2]$ preferentially adopts either the *cis* or *trans* form depending upon the formal oxidation state of the chromium atom:[15] in oxidation states, 0 and II the *cis* isomer is favoured, whilst in oxidation state I the *trans* isomer is preferred. The similar compound $[Cr(CO)_2(dppe\text{-}PP')_2]$ [dppe = 1,2-bis(diphenylphosphino)ethane] exhibits analogous electrochemical behaviour.[22] It is interesting to note that although the $E_{\frac{1}{2}}$ values of the $cis^{+/0}$ redox couples

are similar, those for the *trans*$^{+/0}$ redox couples vary considerably (Table 2).

The oxidative cyclic voltammogram of *cis*-[$Cr(CO)_2$(dppma-*PP'*)$_2$] is shown in Figure 9. On the first forward scan three waves are observed and on the reverse scan a new electrode process is observed at −0.54 V. On the second and subsequent scans (Figure 9) four waves are observed in both directions which can be assigned to the *trans*$^{+/0}$, *cis*$^{2+/1+}$, and the *trans*$^{2+/1+}$ redox couples respectively by analogy with previous studies on *cis*-[$Cr(CO)_2(\eta^2$-L–L$)_2$] (L–L = dppm or dppe).[15,22] The dppa complex *cis*-[$Cr(CO)_2$(dppa-*PP'*)$_2$] showed analogous electrochemical behaviour to the dppma complex. Thus it is concluded that the electrochemical behaviour of the dppa and dppma dicarbonyl complexes is entirely analogous to that of the dppm and dppe dicarbonyl complexes, with all of the redox couples appearing in the same relative order with respect to the $E_{\frac{1}{2}}$ values. The $E_{\frac{1}{2}}$ values and heterogeneous electron-transfer rates are summarized in Table 2.

Conclusions

The tricarbonyl complexes are less easily oxidized than their corresponding dicarbonyl compound (either isomer). This is in agreement with the general behaviour expected of chromium carbonyl complexes.[23]

The rate of heterogeneous electron transfer shows a marked dependence upon the bridging group of the phosphine ligand (Table 2). Electron transfer is significantly slower for the tricarbonyl complexes studied than for the corresponding dicarbonyl complexes (in either isomeric form).

The rate of the disproportionation reaction of the tricarbonyl complexes is also strongly dependent upon the ligand bridging group and is in the order dppm < dppa < dppma. This is the reverse of the electron-transfer rate order, although a larger sample set would be required to confirm a correlation.

The e.s.r. measurements indicate that spin density on the phosphorus atoms is considerable for both the tri- and dicarbonyl complexes.

For the dicarbonyl complexes the standard oxidation potential of the *cis*$^{+/0}$ redox couple appears to remain fairly constant as the phosphine bridge is altered. A much greater range of potential is observed for the *trans*$^{+/0}$ redox couple with the dppm ligand being the easiest to oxidize by a large margin (Table 2).

In all cases the tricarbonyl compounds were found to be very unstable with chromium in oxidation state II. Decomposition of the chromium(II) complexes appears to proceed *via* an intermediate which probably contains only one phosphine ligand, although instead there may remain two phosphine ligands, each behaving in a unidentate fashion. This intermediate has itself only limited stability (concluded from a series of linear-sweep experiments each being preceded by a different length of electrolysis at a potential sufficiently positive as to produce the intermediate species) and following its reduction is seen to undergo very fast further chemical reaction, the final products being solvated chromium(II), free phosphine, and carbon monoxide.

References

1 A. M. Bond, S. W. Carr, and R. Colton, *Inorg. Chem.*, 1984, **23**, 2343 and refs. therein.
2 A. M. Bond, S. W. Carr, and R. Colton, *Organometallics*, 1984, **3**, 541 and refs. therein.
3 M. A. Fox, K. A. Campbell, and E. P. Kyba, *Inorg. Chem.*, 1981, **20**, 4163.
4 A. Blagg, G. R. Cooper, P. G. Pringle, R. Robson, and B. L. Shaw, *J. Chem. Soc., Chem. Commun.*, 1984, 933, and unpublished work.
5 W. Hewertson and H. R. Watson, *J. Chem. Soc.*, 1962, 1490.
6 H. Nöth and L. Meinel, *Z. Anorg. Allg. Chem.*, 1967, **349**, 225.
7 M. Grenness and K. B. Oldham, *Anal. Chem.*, 1972, **44**, 1121.
8 J. C. Imbeaux and J. M. Saveant, *Electroanal. Chem.*, 1973, **44**, 169.
9 L. Nadjo, J. M. Saveant, and D. Tessier, *Electroanal. Chem.*, 1974, **52**, 403.
10 J. M. Saveant and D. Tessier, *Electroanal. Chem.*, 1975, **61**, 251.
11 J. M. Saveant and D. Tessier, *J. Electroanal. Chem. Interfacial Electrochem.*, 1975, **65**, 57.
12 T. Boddington, I. D. Dobson, and N. Taylor, unpublished work.
13 K. B. Oldham, *J. Electroanal. Chem. Interfacial Electrochem.*, 1983, **145**, 9.
14 E. E. Isaacs and W. A. G. Graham, *Inorg. Chem.*, 1975, **14**, 2560.
15 A. M. Bond, R. Colton, and J. J. Jackowski, *Inorg. Chem.*, 1975, **14**, 274.
16 C. Elschenbroich and V. Zenneck, *J. Organomet. Chem.*, 1978, **160**, 125.
17 R. N. Bagchi, A. M. Bond, G. Brain, R. Colton, T. L. E. Henderson, and J. E. Kevebordes, *Organometallics*, 1984, **3**, 4.
18 R. A. Marcus, *Electrochim. Acta*, 1968, **13**, 995.
19 A. J. Bard and L. R. Faulkner, 'Electrochemical Methods—Fundamentals and Applications,' Wiley, New York, 1980, p. 620.
20 A. M. Bond, R. Colton, and J. J. Jackowski, *Inorg. Chem.*, 1975, **14**, 2526.
21 P. S. Braterman, 'Metal Carbonyl Spectra,' Academic Press, London, 1975.
22 F. L. Wimmer, M. R. Snow, and A. M. Bond, *Inorg. Chem.*, 1974, **13**, 1617.
23 B. E. Bursten, *J. Am. Chem. Soc.*, 1982, **104**, 1299.

Received 7th August 1984; *Paper* 4/1394